A LETTERS JOURNAL EXPLORING THE FRONTIERS OF PHYSICS

OFFPRINT

Zipping mechanism for force generation by growing filament bundles

T. KÜHNE, R. LIPOWSKY and J. KIERFELD

EPL, **86** (2009) 68002

TAKE A LOOK AT THE NEW EPL

Europhysics Letters (EPL) has a new online home at
www.epljournal.org

Take a look for the latest journal news and information on:

- reading the latest articles, free!
- receiving free e-mail alerts
- submitting your work to EPL

www.epljournal.org

A Letters Journal Exploring the Frontiers of Physics

June 2009

EPL, **86** (2009) 68002
doi: 10.1209/0295-5075/86/68002

www.epljournal.org

Zipping mechanism for force generation by growing filament bundles

T. Kühne[1], R. Lipowsky[1] and J. Kierfeld[1,2(a)]

[1] *Max Planck Institute of Colloids and Interfaces - Science Park Golm, 14424 Potsdam, Germany, EU*
[2] *Physics Department, TU Dortmund University - 44221 Dortmund, Germany, EU*

received 19 January 2009; accepted in final form 2 June 2009
published online 9 July 2009

PACS 87.16.Ka – Filaments, microtubules, their networks, and supramolecular assemblies
PACS 87.16.A- – Theory, modeling, and simulations
PACS 87.15.rp – Polymerization

Abstract – We investigate the force generation by polymerizing bundles of filaments, which form because of short-range attractive filament interactions. We show that bundles can generate forces by a zipping mechanism, which is not limited by buckling and operates in the fully buckled state. The critical zipping force, *i.e.* the maximal force that a bundle can generate, is given by the adhesive energy gained during bundle formation. For opposing forces larger than the critical zipping force, bundles undergo a force-induced unbinding transition. For larger bundles, the critical zipping force depends on the initial configuration of the bundles. Our results are corroborated by Monte Carlo simulations.

Introduction. – Filamentous polymers play an important role in biological and chemical physics. Both cytoskeletal filaments such as filamentous actin and microtubules and chemically synthesized polymers such as dendronized polymers have diameters in the range from 2 to 25 nanometers which leads to a considerable bending rigidity, *i.e.* the persistence length is comparable or larger than the polymer's contour length. The most important building blocks of the cytoskeleton are actin filaments with a persistence length of $L_p \sim 15\,\mu$m and microtubules with a much larger persistence length $L_p \sim 5\,$mm. Such semiflexible polymers are governed by several competing energy scales in the system: the bending energy and the thermal energy of the filaments, the interaction energy between the filaments, and biochemical forces. In biological systems, such biochemical forces are generated by the activity of molecular motors proteins or the polymerization dynamics of cytoskeletal filaments [1].

Force generation by polymerizing cytoskeletal filaments is essential for various cellular processes, such as motility [1] or the formation of cell protrusions including filopodia, lamellipodia, or acrosomal extensions [2,3], where filaments push against a planar obstacle. Single polymerizing filaments can generate forces in the piconewton range, which arise from the gain in chemical bonding energy upon monomer attachment [4]. This process also involves shape fluctuations of the filament [5], which exerts entropic forces on the planar obstacle [6]. Polymerizing filaments buckle at some critical length under the action of their own polymerization force [7], which limits force generation by single filaments.

Filament bundles support cell protrusions and serve as stress fibres [8,9]. Filament bundles have a higher bending rigidity and are, thus, more stable against buckling if a compressive load is applied [10]. The formation of filament bundles is governed by the competition of thermal fluctuations and attractive interactions, which can arise from crosslinking proteins or unspecific interactions. Crosslinker-mediated interactions allow a reversible formation of actin bundles, which can be regulated by the concentration of crosslinkers in solution [11].

Cellular force generating structures are typically made of polymerizing bundles rather than single filaments. One reason is the enhanced stability of crosslinked stiffer bundles against buckling. Moreover, ensembles of N filaments could share a compressive load force suggesting that the maximally generated force increases by a factor of N, similar to protofilaments in a microtubule [12]. In addition, crosslinking within filament bundles can allow the bundle to generate higher forces by exploiting the additional interaction energy [13,14]. As a result, the mechanism of force generation by polymerizing bundles is difficult

(a) E-mail: Jan.Kierfeld@tu-dortmund.de

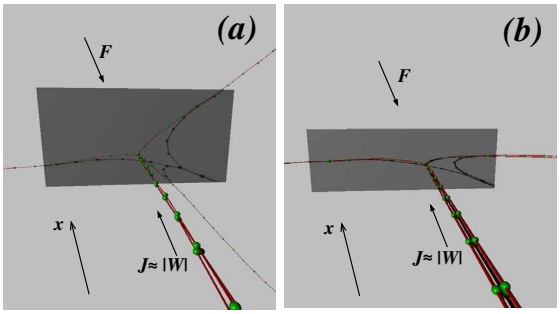

Fig. 1: Snapshots of MC simulations for $N = 3$ filaments close the transition between zipping and force-induced unbinding for for two different initial conditions (a) $b = 123$ and (b) $b = [12]3$.

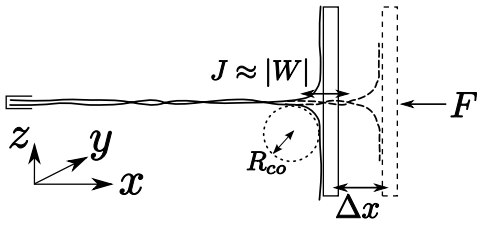

Fig. 2: Zipping mechanism in front of a wall with load force F. Zipping starts in a splayed configuration of filament ends (solid lines). The curvature at the wall is given by the contact radius R_{co}. Zipping a distance Δx (dashed lines) performs a work $F\Delta x$ but gains an adhesive energy $J\Delta x$.

to understand because it involves several types of forces: chemical polymerization forces from monomer bonding, entropic forces from shape fluctuations, and interaction forces. Moreover, a critical buckling force limits the mechanical stability of filaments. In this letter, we show that there exists one possible mechanism of force generation by filament bundles, the so-called *zipping mechanism*, which is completely based on the conversion of adhesive filament interaction energy into force and which operates if individual filaments within a bundle are fully buckled in front of an obstacle as shown in fig. 1. The force generated by this mechanism is independent of chemical energy and entropic forces and is *not* limited by buckling. We characterize this zipping mechanism quantitatively and also show its intimate relation to a force-induced unbinding transition of filament bundles.

Bundle model. – In order to model a single bundle of N filaments we start from an effective Hamiltonian containing bending energies and interaction energies of all filaments,

$$\mathcal{H} = \sum_{i=1}^{N} \mathcal{H}_{b,i} + \sum_{i,j=1}^{N} \mathcal{H}_{2,ij}. \tag{1}$$

In the first term, $\mathcal{H}_{b,i} = \int_0^{L_i} \mathrm{d}s \frac{1}{2}\kappa(\partial_s \mathbf{t}_i)^2$ is the bending energy of filament i with bending rigidity κ and contour length L_i, which is parametrized by its arclength s with a contour $\mathbf{r}_i(s)$ and unit tangent vectors $\mathbf{t}(s) \equiv \partial_s \mathbf{r}_i$. We consider filaments with identical κ and, thus, identical persistence lengths $L_p \equiv \kappa/k_B T$ at temperature T. The second term describes attractive pairwise interactions between the filaments, $\mathcal{H}_{2,ij} = \int_0^{\min(L_i,L_j)} \mathrm{d}s[V_\mathrm{r}(\mathbf{\Delta r}_{ij}) + V_\mathrm{a}(\mathbf{\Delta r}_{ij})]$, where $\mathbf{\Delta r}_{ij} = \mathbf{r}_i(s) - \mathbf{r}_j(s)$ is the distance between filaments i and j at arclength s along the filament. We assume that only monomers with similar arclength parameters interact. The first term is the hard-core repulsion of filaments with a potential $V_\mathrm{r}(\mathbf{r}) = \infty$, for $|\mathbf{r}| < \ell_\mathrm{r}$ and $V_\mathrm{r}(\mathbf{r}) = 0$, otherwise, where ℓ_r is of order of the filament diameter. The second term is an short-range attractive potential $V_\mathrm{a}(\mathbf{r})$, which we model by a potential well: the filament can gain an additional energy $|W|$ over a range ℓ_a,

$$V_\mathrm{a}(\mathbf{r}) = \begin{cases} -|W|, & \ell_\mathrm{r} \leqslant |\mathbf{r}| < \ell_\mathrm{r} + \ell_\mathrm{a}, \\ 0, & \text{otherwise.} \end{cases} \tag{2}$$

For cytoskeletal filaments, the attractive potential V_a typically arises from linker-mediated attractions. Then its strength $|W|$ is proportional to the crosslinker concentration in solution and the potential range ℓ_a is of the order of a linker size. In the absence of forces and filament polymerization, bundles of N filaments form in a single discontinuous bundling transition at a critical potential strength $W_c^{(N)}$ [11,15].

In the following we will consider bundles of polymerizing filaments which exert forces onto a planar wall. We apply clamped and capped boundary conditions on one end of the bundle ($s = 0$), where all filaments are oriented into the x-direction and cannot polymerize or depolymerize. Because of the filament bending rigidity this induces a preferred orientation of the bundle into the x-direction, see fig. 2. Initially, the capped ends $s = 0$ of filaments are positioned in proximity. The contour lengths L_i of filaments can differ because of the polymerization process. Monomers of length Δl can attach and detach to and from filaments at the other end ($s = L$) giving rise to changes in the contour length $\Delta L = \pm\Delta l$. The attachment of monomers leads to a polymerization energy gain $E_p < 0$, which is related to the ratio $\omega_\mathrm{on}/\omega_\mathrm{off} = e^{-E_p/k_B T}$ of monomer attachment and detachment rates. The attachment rate ω_on is proportional to the monomer concentration in the surrounding solution and, thus, also the polymerization energy E_p is controlled by monomer concentration. We assume a constant monomer concentration throughout the polymerization process, which implies a constant on-rate ω_on and, thus, constant E_p.

We will consider growth against a rigid planar wall in the yz-plane perpendicular to the average filament orientation. The wall can move in the x-direction but cannot rotate. The wall is loaded with an additional force F. We are not addressing ratchet mechanisms involved in the insertion of monomers at the loaded end of the filament in the proximity of the wall [4,5]. Therefore,

we assume that the wall has a very small diffusion coefficient such that it moves instantaneously with the position of the monomer with the maximal x-coordinate $x_{\max}$. Changes $\Delta x_{\max}$ give rise to an additional energy $F\Delta x_{\max}$ for the filament. If a monomer is attached such that $\Delta x_{\max} > 0$, this leads to a change in the attachment rate $\omega_{\rm on} = e^{-(E_p + F\Delta x_{\max})/k_B T}\omega_{\rm off}$, where we assume that the value of $\omega_{\rm off}$ is unaffected by force. Then growth stalls for $F = |E_p|/\Delta x_{\max}$. The specific values of $\omega_{\rm on,off}$ are not essential, we only assume that shape fluctuations of the filaments are faster than their growth dynamics. In addition, shape fluctuations can give rise to changes in $\Delta x_{\max}$ and corresponding energy changes.

Buckling of single growing filaments. – A single cytoskeletal filament can generate forces in the piconewton range [4,5]. The polymerization force is defined by the corresponding load force that stalls polymerization. For a single filament this polymerization force is directly related to the polymerization energy E_p per monomer, $F_p = |E_p|/\Delta l$. Polymerizing filaments will buckle if the load force F exceeds the critical force for buckling, $F_b \sim \kappa/L^2$. In the following we will discuss the possible dynamically stable steady states of growing or shrinking filaments.

For small load forces $F < F_p$, the filament will grow, and the critical force for buckling, $F_b \sim \kappa/L^2$, decreases. Eventually, the load force F becomes larger than F_b, and the filament buckles [7]. After buckling, the growing filament end at $s = L$ has an angle $\phi_L > 0$ with the x-axis, and the polymerization force is opposed by the reduced load force $F\cos\phi_L$ in the direction tangential to the filament. This will lead to further growth, and the only stable state of a growing filament is the fully buckled state with $\phi_L = \pi/2$. Upon increasing the load force such that $F\cos\phi_L > F_p$, the filament shrinks. We find that the buckled state of a shrinking filament with $F_p = F\cos\phi_L < F$ represent an *unstable* mechanical equilibrium because ϕ_L is increasing for increasing L at fixed load force F. For flexible walls, a similar instability has been discussed in ref. [16]. Therefore, the only stable states of a shrinking filament are the unbuckled state ($\phi_L = 0$) and the fully buckled state ($\phi_L = \pi/2$) as long as the length reservoir is sufficiently large. Because growing filaments will always end up in a fully buckled state, mechanisms for force generation which also operate in the fully buckled state of individual filaments are essential in systems containing polymerizing filaments. We will demonstrate that filament bundles can generate forces using a zipping mechanism if each filament in the bundle is fully buckled.

Zipping and force-induced unbinding. – Cells usually rely on bundles of several filaments for the formation of cell protrusions such as filopodia or acrosomal extensions. Such bundles have a higher bending rigidity [10] and are more stable against buckling. Stall forces of polymerizing actin bundles could be determined experimentally only recently [17]. If the force generation mechanism is based on the polymerization energy E_p of single filaments, bundles of filaments are believed to have higher stall forces because of load sharing. It has been proposed that within bundles filaments can additionally exploit an attractive interaction to generate higher forces [13,14].

Within this letter, we quantitatively investigate the interplay of attractive bundling interactions and external load force. We find that it is possible to generate forces independently of the polymerization energy E_p and entirely based on the attractive interaction between filaments by a zipping mechanism. In this mechanism, the adhesive energy which is gained during bundle formation generates a zipping force.

We will first explain the mechanism for two filaments. As shown in fig. 2, zipping of two filaments requires a particular initial condition, a "zipping fork", where both filaments are in a fully buckled state with $\phi_L = \pi/2$ and well-separated uncapped filament ends at the wall in a splayed configuration. As explained above, the fully buckled state is generic for polymerizing non-interacting filaments. The splayed initial condition arises then naturally by the thermal motion of uncapped filaments ends if the capped ends are anchored in proximity and the crosslinker concentration or the adhesive potential is increased from low values ($|W| < |W_c^{(2)}|$). The wall exerts a total force F in the negative x-direction. If the two filaments bind together along an additional length Δx, the bundle gains the free energy $J\Delta x$, where $J > 0$ represents the free energy of bundling, which arises from the competition of thermal shape fluctuations of filaments and the short-range attraction between filaments [11]. This implies that the zipping mechanism will only work in the bundled phase. In the absence of thermal fluctuations, we have $J = |W|$, *i.e.* the bundling free energy J equals the potential interaction energy gain $|W|$. In the presence of thermal shape fluctuations, the potential energy is reduced by entropic contributions. Close to the discontinuous unbinding transition, the free energy vanishes according to $J \sim |W_c^{(2)} - W|$ [11]. If the filaments bind together along an additional length Δx, the wall has to move the same distance Δx against the load force F. This movement performs a work $F\Delta x$, and the total free energy gain is

$$\Delta G = (J - F)\Delta x, \tag{3}$$

see fig. 2. If the load force F is smaller than the critical force $F_c^{(2)} = J$, a change $\Delta x > 0$ of the bound length leads to a free energy gain $\Delta G > 0$ resulting in spontaneous *zipping*. The critical force $F_c^{(2)}$ represents the maximal force which can be generated by the zipping mechanism for two filaments. For forces $F > F_c^{(2)} = J$, an "inverse" zipping with $\Delta x < 0$ leads to a free energy gain, *i.e.* the bundle is separated by the load force F. This process represents a *force-induced unbinding*. Deep inside the bundled phase, *i.e.* for $|W| \gg |W_c^{(2)}|$, we find critical

forces $F_c^{(2)} = J \approx |W|$. Close to the thermal unbinding transition the critical zipping force vanishes as $F_c^{(2)} = J \sim |W_c^{(2)} - W|$.

We can also consider zipping and force-induced unbinding as a function of the potential strength W for fixed force F. Force-induced unbinding then happens for $|W|$ smaller than a force-dependent critical potential strength $W_c^{(2)}(F)$, which is given by $|W_c^{(2)}(F)| \approx F$ deep in the bundled phase, where large forces are needed to unbind the bundle, and approaches the critical potential strength for purely thermal unbinding, $W_c^{(2)}(F) \approx W_c^{(2)} - F$, for small forces. Zipping takes place above the critical potential strength for $|W| > W_c^{(2)}(F)$.

All zipping and force-induced unbinding thresholds are independent of the polymerization energy E_p and, thus, these phenomena do not depend on the presence of the polymerization force. The zipping mechanism exploits the binding free energy J between filaments. The polymerization at the end of the filaments is needed only to provide a sufficient reservoir of length for the bundle such that force can be generated continuously. The polymerization has to be sufficiently fast to establish a length reservoir but the details of the polymerization kinetics are not important for the zipping mechanism.

The mechanism requires the separation of filament ends in the splayed zipping fork configuration in order to avoid binding of filaments by rotation around the x-axis without any force generation. This separation is maintained by the slow kinetics of the long polymer ends or by fixing the filament ends in the yz-plane. In the splayed configuration semiflexible filaments attain a radius of curvature at the wall, which is given by the contact radius $R_{co} \sim (\kappa/J)^{1/2}$ [18], see fig. 2. The stiffness of filaments is important in order to allow for a force transmission onto the wall by the curved contact segments. Only filaments with a nonzero bending rigidity can exert a torque onto the wall in the fully buckled state.

Monte Carlo simulations. – In order to gain further insight into zipping and force-induced unbinding for $N \geqslant 2$ filaments we have performed Monte Carlo (MC) simulations for identical filaments using the effective Hamiltonian (1). Simulation snapshots are shown in fig. 1. In the MC simulation we use a discretized parameterization in terms of the arc length s as in the worm-like chain model $\mathcal{H}_{b,i} = \int_0^{L_i} \mathrm{d}s \frac{1}{2}\kappa(\partial_s \mathbf{t})^2$ and model the constraint $|\mathbf{t}(s)| = 1$ by a sufficiently stiff harmonic potential. The contours $\mathbf{r}_i(s)$ of each filament i of length L_i are discretized into $M_i = L_i/\Delta s$ equidistant points $\mathbf{r}_i^n = \mathbf{r}_i(n\Delta s)$. The total energy $\mathcal{H} = \sum_i \mathcal{H}_{b,i} + \sum_{i,j} \mathcal{H}_{2,ij}$ is calculated using a discretized bending energy $\mathcal{H}_{b,i} = \sum_{n=1}^{M_i} \kappa\big(1 - \hat{\mathbf{r}}_i^{n-1,n} \cdot \hat{\mathbf{r}}_i^{n,n+1}\big) + k(|\mathbf{r}_i^{n,n+1}| - \Delta s)^2$, where $\mathbf{r}_i^{n-1,n} \equiv \mathbf{r}_i^n - \mathbf{r}_i^{n-1}$ and $\hat{\mathbf{r}}_i^{n-1,n} \equiv \mathbf{r}_i^{n-1,n}/|\mathbf{r}_i^{n-1,n}|$, and the second term represents the spring energy that enforces the constraint $|\mathbf{t}_i(s)| = 1$ in the discretized model (we use $k = 100 k_B T/\Delta s^2$). We also discretize the attractive interaction energy according to $\mathcal{H}_{2,ij} = \sum_{n=1}^{\min M_i, M_j} [V_\mathrm{r}(\mathbf{r}_{ij}^n) + V_\mathrm{a}(\mathbf{r}_{ij}^n)]$. The effects of monomer attachment and detachment and the load force can be taken into account by additional energy contributions $\mathcal{H}_p = E_p \sum_i M_i$ and $\mathcal{H}_F = F x_{\max}$.

We employ the Metropolis algorithm for the total energy $\mathcal{H} + \mathcal{H}_p + \mathcal{H}_F$. For configurational equilibration we offer local displacement moves of the vectors $\mathbf{r}_i^n$ in each MC step and pivot moves of whole filament segments. In addition we attempt attachment and detachment moves of monomers with smaller frequency in order to achieve shape fluctuations of filaments which are faster than the growth dynamics. For a fast equilibration for longitudinal fluctuations of the bound or zipped length along the filament we also attempt reptation-like moves where monomers are transferred between the capped end at $s = 0$ and the uncapped end at $s = L_i$ and vice versa; these moves do not change the total number of monomers. The zipping mechanism relies on the separation of filament ends into a split zipping fork configuration at the wall, see fig. 1. Filament ends have to stay separated in order to avoid binding of filaments by simple rotation. In the MC simulations such rotations are kinetically suppressed as the rotational diffusion of a whole filament by local displacement moves happens on much larger time scales as zipping, which is accelerated in the MC simulations by the reptation-like moves.

Force-induced unbinding transition. – We first consider the force-induced unbinding transition of filament bundles. In fig. 3, we show MC results for the average binding energy per length and per filament, $\langle e_2 \rangle \equiv \langle (\sum_{i,j=1}^N \mathcal{H}_{2,ij})/(\sum_{i=1}^N L_i) \rangle$, for bundles with $N = 3$ and $N = 4$ in the presence of a load force F and as a function of the potential strength per length $|W|$.

In the absence of external forces, a single, discontinuous unbinding transition occurs at a critical potential strength $W_c^{(N)}$, which only depends on the number of filaments in the bundle [11]. In the presence of a load force, on the other hand, the unbinding transition occurs i) in several steps, ii) at critical potential strengths, which depend on the load force, and iii) via different pathways depending on the initial subbundle configuration. The number of transition steps and the critical potential strengths in force-induced unbinding depend on the initial zipping fork configuration, in particular on the number and types of subbundles in the initial splayed configuration. For $N > 2$ filaments several initial subbundle configurations are possible. We will focus on conditions deep in the bundled phase of N filaments. Then, starting with high potential strengths $|W|$, we first find a force-induced unbinding of subbundles at a critical potential strength $|W_c^{(N|b)}(F)| \approx F/n(N|b)$, where b will index the initial subbundle configuration and with a number $n(N|b)$ of pairwise filaments interactions lost upon subbundle unbinding. Then, at smaller critical potential strengths $|W_c^{(M)}|$, there is a subsequent thermal unbinding transition of subbundles containing M filaments, which is independent of force.

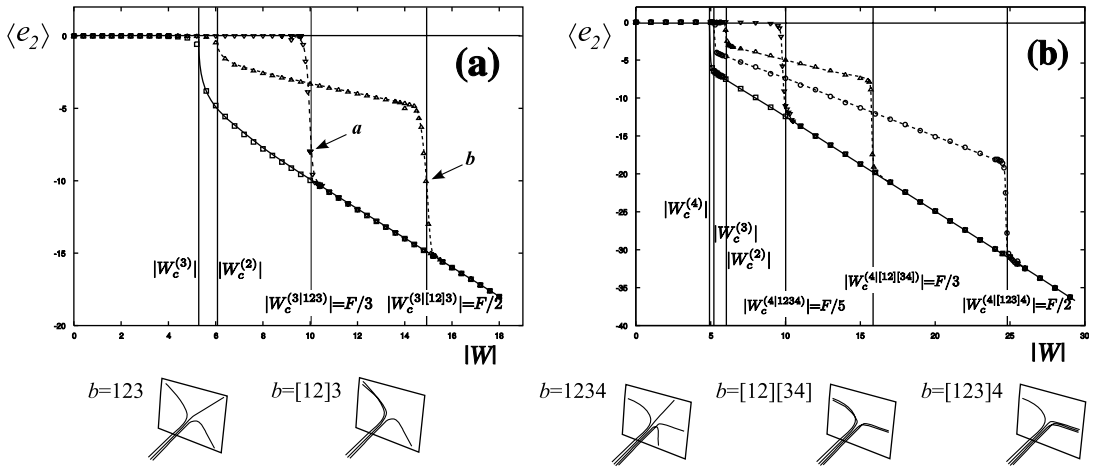

Fig. 3: MC data for the average binding energy per filament and per length, $\langle e_2 \rangle$ as a function of the potential strength $|W|$ for (a) $N=3$ and (b) $N=4$ identical filaments (with persistence length $L_p=100$, initial contour length $L=100$, potential range $\ell_a=0.001$ and hard-core radius $\ell_r=0.1$; all lengths in units of Δl; energies in units of k_BT; lines are guides to the eye). Arrows correspond to the snapshots in fig. 1. In the absence of an external force $F=0$ ($\square$), the thermal unbinding transition happens at a critical potential strength $|W_c^{(N)}|$. (a) For $N=3$ an external force $F=30$ is applied. For an initial configuration $b=123$ ($\triangledown$), the unbinding transition occurs at a critical potential strength $|W_c^{(3|123)}| \approx F/3$. For an initial condition $b=[12]3$ ($\triangle$), a cascade of two unbinding transition occurs at critical potential strengths $|W_c^{(2)}|$ and $|W_c^{(3|[12]3)}| \approx F/2$. (b) For $N=4$ filaments an external force $F=50$ is applied. This leads to three different force-dependent critical potential strengths $|W_c^{(4|1234)}| \approx F/5$ ($\triangledown$), $|W_c^{(4|[123]4)}| \approx F/3$ ($\circ$), and $|W_c^{(4|[12][34])}| \approx F/2$ ($\triangle$) depending on the initial subbundle configuration.

For a bundle with $N=3$ filaments, two different initial zipping fork configurations and, thus, two force-induced unbinding pathways are possible, see fig. 3(a). In configuration $b=123$, all three filaments point in different directions. In configuration $b=[12]3$, the end of the bundle is split into one subbundle of two bound filaments [12] and the third filament 3 pointing in a different direction. In configuration $b=123$, there is a single unbinding transition at $|W_c^{(3|123)}| \approx F/3$ with $n(3|123)=3$ pairwise filament interactions lost upon unbinding. In configuration $b=[12]3$, on the other hand, there are two unbinding transitions: First, filament 3 is separated from the subbundle [12] at $|W_c^{(3|123)}| \approx F/2$ because $n(3|123)=2$ pairwise filament interactions are lost upon subbundle unbinding. Further decreasing the potential strength $|W|$, there is a second thermal unbinding transition of the subbundle [12] at the critical value $|W_c^{(2)}|$, which is independent of force. The values for $n(3|b)$ correspond to a triangular arrangement of a three filament bundle, as can be seen in fig. 1.

For bundles with $N>3$ even more initial subbundle configurations are possible giving rise to a variety of possible force-induced unbinding pathways. In fig. 3(b), we show MC results for a bundle with $N=4$ filaments, which exhibits already three different unbinding pathways under force. These pathways are related to the initial configurations $b=1234$ with four separated filaments, $b=[12][34]$ with two subbundles containing two filaments each, and $b=[123]4$ with one subbundle containing three filaments and one separated filament. The numbers of pairwise filament interactions lost upon unbinding are $n(4|1234)=5$, $n(4|[12][34])=3$, and $n(4|[123]4)=2$. All three values for $n(4|b)$ can be explained by a triangular arrangement of filaments in the bundle, as it has been observed for equilibrium bundles in ref. [11]. After force-induced unbinding, the remaining subbundles unbind thermally at lower critical potential strengths in a second transition.

Zipping. – Whereas a bundle of N filaments unbinds for $|W| < W_c^{(N|b)}(F)$, it starts zipping above the critical potential strength, for $|W| > W_c^{(N|b)}(F)$. The filament can generate and transmit forces onto a wall by the zipping mechanism, which converts adhesive energy into a force. The critical force $F_c^{(N|b)}$ is the maximal force that a bundle with N filaments and initial conditions k can generate by the zipping mechanism for a given potential strength $|W|$. The critical forces $F_c^{(N|b)}$ for zipping with an initial condition b are related to the critical potential strengths $W_c^{(N|b)}(F)$ for force-induced unbinding by $W_c^{(N|b)}(F_c^{(N|b)}) = |W|$, which gives $F_c^{(N|b)} \approx |W|/n(N|b)$ at high potential strengths. Therefore, we also find different critical zipping forces depending on the zipping pathway, which is determined by the initial configuration b.

The kinetics of zipping in the MC simulation is characterized by the average velocity $\langle v_w \rangle$ of the wall along the x-axis in the stationary state. For a given load force F, the velocity $\langle v_w \rangle$ changes sign at the critical potential strength $W_c^{(2)}(F) \approx F$ with $\langle v_w \rangle < 0$ for force-induced unbinding for $|W| < W_c^{(2)}(F)$ and $\langle v_w \rangle > 0$ for

zipping for $|W| > W_c^{(2)}(F)$. The average velocity is given by $\langle v_w \rangle = (\omega_+ - \omega_-)\Delta l$ in terms of the rates ω_+ and ω_- for zipping and unzipping a segment of length Δl. These rates depend on the attempted MC moves, and their sum $\omega_0 = \omega_+ + \omega_-$ is given by the frequency at which reptation-like moves are offered in the MC dynamics. Furthermore, eq. (3) leads to $\omega_+/\omega_- = \exp[(J-F)\Delta l/k_BT]$ with $J - F \approx |W| - |W_2^{(2)}(F)|$, such that

$$\langle v_w \rangle \approx v_0 \tanh\left(\frac{(|W| - |W_2^{(2)}(F)|)\Delta l}{2k_BT}\right) \qquad (4)$$

with a maximal velocity $v_0 = \omega_0 \Delta l$. This result is in agreement with results from our MC simulations (data not shown) and shows that the width of the transition between force-induced unbinding an zipping decreases with decreasing temperature T.

In the MC kinetics we neglect frictional forces, which limit reptation-like motion. In a real system we expect the result (4) for the velocity-potential relation to hold for $|\langle v_w \rangle| \ll v_0$, *i.e.*, close to equilibrium with a maximal velocity v_0, which is determined by the equilibrium between zipping force and frictional force of the polymer ends.

Discussion and conclusion. – We have shown that forces can be generated by a zipping mechanism, which is completely based on the conversion of adhesive filament interaction energy into force and which operates independently of the polymerization energy if filaments within a bundle are fully buckled. Below a critical potential strength or above a critical load force zipping does no longer occur, and there is a transition from zipping to a force-induced unbinding of the filament bundle.

The resulting zipping force is given by the filament interaction energy per length which is liberated upon separating the filaments. For F-actin crosslinkers such as α-actinin or filamin recent measurements give binding energies of $4k_BT$ per crosslinker and filament pair [19], which yields zipping forces $F_c^{(2)} \simeq 6\,\mathrm{pN}$ for two filaments if we assume one crosslinker per actin monomer. Actin filaments can also be bundled by counterions with typical binding energies of $0.02k_BT$ per actin monomer for magnesium ions [20], which are much weaker than protein crosslinkers. For these interactions bundles of the order of $N = 10$ filaments are needed to generated zipping forces in the piconewton range if we assume a triangular filament arrangement and separation into single filaments resulting in $n^{(N|b)} \approx 3N$ for large N.

The zipping mechanism only relies on adhesive energy and does not require a large variety of regulatory proteins as found for actin-based motility of eukaryotic cells [21,22]. Zipping mechanisms may also contribute to force generation in the presence of regulatory proteins, in particular, force generation by filament bundles in cell protrusions such as filopodia [23] but they could play a more prominent important role for the motility of relatively primitive cells such as sperm cells of nematodes [14,24,25]. Zipping mechanisms could also be exploited to create artificial force generating systems using synthetic semiflexible polymers with attractive interactions.

* * *

We acknowledge financial support within the Collaborative Research Center Mesoscopically Structured Composites (SFB 448) of the Deutsche Forschungsgemeinschaft.

REFERENCES

[1] Bray D., *Cell Movements: From Molecules to Motility*, Vol. **2** (Garland Publishing) 2001.
[2] Theriot J. A., *Traffic*, **19** (2000) 1.
[3] Mogilner A., *Curr. Opin. Cell Biol.*, **18** (2006) 32.
[4] Peskin C., Odell G. M. and Oster G. F., *Biophys. J.*, **65** (1993) 316.
[5] Mogilner A. and Oster G., *Biophys. J.*, **71** (1996) 3030.
[6] Gholami A., Wilhelm J. and Frey E., *Phys. Rev. E*, **74** (2006) 041803.
[7] Dogterom M. and Yurke B., *Science*, **278** (1997) 856.
[8] Bartles J. R., *Curr. Opin. Cell Biol.*, **12** (2000) 72.
[9] Faix J. and Rottner K., *Curr. Opin. Cell Biol.*, **18** (2006) 18.
[10] Bathe M., Heussinger C., Claessens M. M. A. E., Bausch A. R. and Frey E., *Biophys. J.*, **94** (2008) 2955.
[11] Kierfeld J., Kühne T. and Lipowsky R., *Phys. Rev. Lett.*, **95** (2005) 038102.
[12] Sander van Doorn G., Tănase C., Mulder B. M. and Dogterom M., *Eur. Biophys. J*, **29** (2000) 2.
[13] Mahadevan L. and Matsudaira P., *Science*, **288** (2000) 95.
[14] Mogilner A. and Oster G., *Science*, **302** (2003) 1340.
[15] Kierfeld J. and Lipowsky R., *Europhys. Lett.*, **62** (2003) 285.
[16] Daniels D. R., Marenduzzo D. and Turner M. S., *Phys. Rev. Lett.*, **97** (2006) 098101.
[17] Footer M. J., Kerssemakers J. W. J., Theriot J. A. and Dogterom M., *Proc. Natl. Acad. Sci. U.S.A.*, **104** (2007) 2181.
[18] Kierfeld J., *Phys. Rev. Lett.*, **97** (2006) 058302.
[19] Ferrer J. M., Lee H., Chen J., Pelz B., Nakamura F., Kamm R. D. and Lang M. J., *Proc. Natl. Acad. Sci. U.S.A.*, **105** (2008) 9221.
[20] Tang J. X., Käs J. A., Shah J. V. and Janmey P. A., *Eur. Biophys. J.*, **30** (2001) 477.
[21] Pollard T., *Nature*, **422** (2003) 741.
[22] Carlier M.-F., LeClainche C., Wiesner S. and Pantaloni D., *BioEssays*, **25** (2003) 336.
[23] Mogilner A. and Rubinstein B., *Biophys. J.*, **89** (2005) 782.
[24] Miao L., Vanderlinde O., Stewart M. and Roberts T. M., *Science*, **302** (2003) 1405.
[25] Roberts T. M. and Stewart M., *J. Cell Biol.*, **149** (2000) 7.